

## Diffusion coefficient of $^{113}\text{Sn}$ , $^{124}\text{Sb}$ , $^{110m}\text{Ag}$ , and $^{195}\text{Au}$ in liquid Sn

A. Bruson and M. Gerl

*Laboratoire de Physique des Solides de Nancy I,\* C. O. 140, 54037 Nancy Cedex, France*

(Received 21 November 1979)

Measurements of the diffusion coefficient of  $^{113}\text{Sn}$ ,  $^{124}\text{Sb}$ ,  $^{110m}\text{Ag}$ , and  $^{195}\text{Au}$  in liquid Sn have been made using a shear cell assembly which provides accurate data. The experimental diffusion coefficient is given by  $D_i = CD_i^E$ , where  $D_i^E$  is obtained using Enskog's theory and  $C$  is a correction factor accounting for dynamical effects.  $C$  is strongly dependent on the density of the fluid and on the relative mass and size of the solute with respect to the solvent. The data show that (i) the density effects in self-diffusion are qualitatively in good agreement with molecular-dynamics calculations; (ii) for impurity diffusion,  $C$  decreases with the mass of the solute, whatever the density, as predicted by molecular-dynamics (MD) calculations; (iii) size effects on  $C$  are in agreement with MD calculations for impurities larger than the solvent; and (iv) Ag and Au solutes exhibit anomalously large values of  $C$  which may be due to valence effects.

### I. INTRODUCTION

As we recalled in a previous paper<sup>1</sup> self-diffusion and impurity diffusion in liquid metals are qualitatively well understood. Enskog's theory of dense fluids<sup>2</sup> provides a diffusion coefficient  $D_i^E$  of the test particle which is of the right order of magnitude. Alder *et al.*<sup>3,4</sup> have corrected this theory to account for dynamical corrections. Hence the diffusion coefficient  $D_i$  of a species  $i$  in a liquid is usually written

$$D_i = C_i D_i^E. \quad (1)$$

As shown by Alder *et al.*, the correlation factor  $C_i$  depends on the fluid density and on the relative mass and size of the solute with respect to the solvent.

In our previous paper<sup>1</sup> we investigated the diffusion properties of some solute atoms in liquid copper and we compared the experimental results to molecular dynamics calculations on hard-sphere systems. According to the mass and size of the solute, two correlation regimes can be observed: (i) for particles larger and heavier than the solvent (e.g., Sn, Sb, Ag, and Au in liquid Cu),  $C_i$  increases as the mass and/or size of the solute atoms increases and (ii) for solute atoms smaller and of smaller mass than the solvent,  $C_i$  increases as the mass of the diffusing particle increases and as its hard-sphere diameter is reduced.

In order to test this behavior, we have measured the diffusion coefficient of  $^{113}\text{Sn}$ ,  $^{110m}\text{Ag}$ ,  $^{124}\text{Sb}$ ,  $^{195}\text{Au}$  in liquid Sn in a larger density range ( $1.56 < V/V_0 < 2.6$ ) than was technically possible in liquid copper ( $1.56 < V/V_0 < 1.75$ ).  $V$  is the molar volume of the liquid at the temperature of the experiment and  $V_0$  is its close-packed value. In Sec. II we describe the experimental technique and we give the experimental data. Section III is de-

voted to the analysis of the dependence of the correlation factor on the fluid density and on the hard-sphere parameters of the solute atoms.

### II. EXPERIMENTAL METHOD AND RESULTS

In order to avoid most of the drawbacks presented by the capillary reservoir technique which is usually employed to measure diffusion coefficients, a shear cell has been constructed and is described with some details in Ref. 1. At the beginning of the run, a thin layer of a radioisotope of the solute is put in contact with a capillary of the solvent metal. When the diffusion run is completed, each disk of the shear cell is rotated with respect to its neighbors. This operation, which takes place at the diffusion temperature, accurately determines the end of the diffusion experiment, and prevents any redistribution of solute when the capillary is cooled down to room temperature. The sections of the sample are subsequently extracted from the disks and their radioactivity is measured using a standard NaI-Tl analyzer. The diffusion coefficient is obtained by a least-squares fitting of the experimental concentration profile to the solution of the appropriate Fick equation.

Using this technique, we have measured the diffusion coefficient of the radioisotopes  $^{110m}\text{Ag}$ ,  $^{113}\text{Sn}$ ,  $^{124}\text{Sb}$ , and  $^{195}\text{Au}$  in liquid tin in a temperature range of about 1300 K above the melting point, which corresponds to the density range  $1.56 < V/V_0 < 2.60$ . The experimental data are recorded in Table I and compared with the results given by different authors in Figs. 1 and 2.

In order to make a comparison between the diffusion coefficients of the four isotopes investigated in the present work, and for reasons given in Sec. III of our previous paper,<sup>1</sup> we consider

TABLE I. Diffusion coefficients of  $^{110m}\text{Ag}$ ,  $^{113}\text{Sn}$ ,  $^{124}\text{Sb}$ , and  $^{195}\text{Au}$  in liquid tin.

$^{110m}\text{Ag}$		$^{113}\text{Sn}$		$^{124}\text{Sb}$		$^{195}\text{Au}$	
$T$ (K)	$D$ ( $10^{-5} \text{ cm}^2 \text{ s}^{-1}$ )	$T$ (K)	$D$ ( $10^{-5} \text{ cm}^2 \text{ s}^{-1}$ )	$T$ (K)	$D$ ( $10^{-5} \text{ cm}^2 \text{ s}^{-1}$ )	$T$ (K)	$D$ ( $10^{-5} \text{ cm}^2 \text{ s}^{-1}$ )
621	$3.8 \pm 0.2$	628	$3.4 \pm 0.2$	589	$2.6 \pm 0.1$	693	$5.2 \pm 0.3$
693	$5.6 \pm 0.3$	700	$4.2 \pm 0.2$	624	$2.9 \pm 0.2$	826	$6.7 \pm 0.3$
826	$7.1 \pm 0.4$	825	$5.5 \pm 0.3$	630	$3.0 \pm 0.2$	1108	$10.8 \pm 0.5$
943	$10.2 \pm 0.5$	973	$7.4 \pm 0.4$	743	$4.4 \pm 0.2$	1323	$15.1 \pm 0.8$
1108	$11.8 \pm 0.6$	1050	$8.4 \pm 0.4$	841	$6.4 \pm 0.3$	1428	$15.7 \pm 0.8$
1428	$17.2 \pm 0.9$	1100	$8.9 \pm 0.5$	891	$6.7 \pm 0.3$	1538	$20.5 \pm 1.0$
1538	$21.0 \pm 1.0$	1300	$11.3 \pm 0.6$	1100	$7.6 \pm 0.4$	1683	$22.1 \pm 1.1$
1683	$22.0 \pm 1.1$	1450	$13.2 \pm 0.7$	1400	$11.8 \pm 0.6$	1853	$26.1 \pm 1.3$
1853	$25.2 \pm 1.3$	1520	$13.9 \pm 0.7$	1705	$15.0 \pm 0.8$		
		1600	$14.9 \pm 0.8$				
		1925	$19.0 \pm 1.0$				

that  $D$  varies as a function of temperature:

$$D = A(T - T_m) + D_m, \quad (2)$$

where  $D_m$  is the diffusion coefficient linearly extrapolated to the melting temperature  $T_m$  ( $T_m = 504.9$  K). The values obtained for the parameters  $A$  and  $D_m$  are recorded in Table II.

### III. INTERPRETATION

Using the result given by Thorne,<sup>2,15</sup> the binary collision diffusion coefficient  $D_i^E$  of the solute  $i$  in the solvent labeled  $s$  can be written in the Enskog approximation

$$D_i^E = \frac{3}{8n\sigma_{is}^2 g_{is}(\sigma_{is})} \left( \frac{kT}{2\pi\mu} \right)^{1/2}, \quad (3)$$

where  $\mu = m_i m_s / (m_i + m_s)$  is the reduced mass,  $\sigma_i$ ,  $\sigma_s$  are the hard-sphere diameters of solute and solvent atoms, respectively,  $\sigma_{is} = \frac{1}{2}(\sigma_i + \sigma_s)$ , and  $g_{is}(\sigma_{is})$  is the radial distribution function of unlike atoms at contact. In order to calculate  $D_i^E$ , we must therefore know  $\sigma_i$  and  $\sigma_s$  and  $g_{is}(\sigma_{is})$ . We now briefly describe our method for determining these quantities.

#### A. Hard-sphere diameters

In his work on liquid metals<sup>16,17</sup> Protopapas showed that the self-diffusion coefficient can be accurately predicted if each atom  $\alpha$  is considered as a hard sphere with a diameter  $\sigma_\alpha(T)$  depending on temperature according to the law

$$\sigma_\alpha(T) = 1.288 \left( \frac{M_\alpha}{\rho_{\alpha m}} \right)^{1/3} \left[ 1 - 0.112 \left( \frac{T}{T_{\alpha m}} \right)^{1/2} \right], \quad (4)$$

where  $\rho_{\alpha m}$  is the mass density at melting temperature  $T_{\alpha m}$ . Using this equation, we can calculate the diameters  $\sigma_i(T)$  and  $\sigma_s(T)$  at any temperature

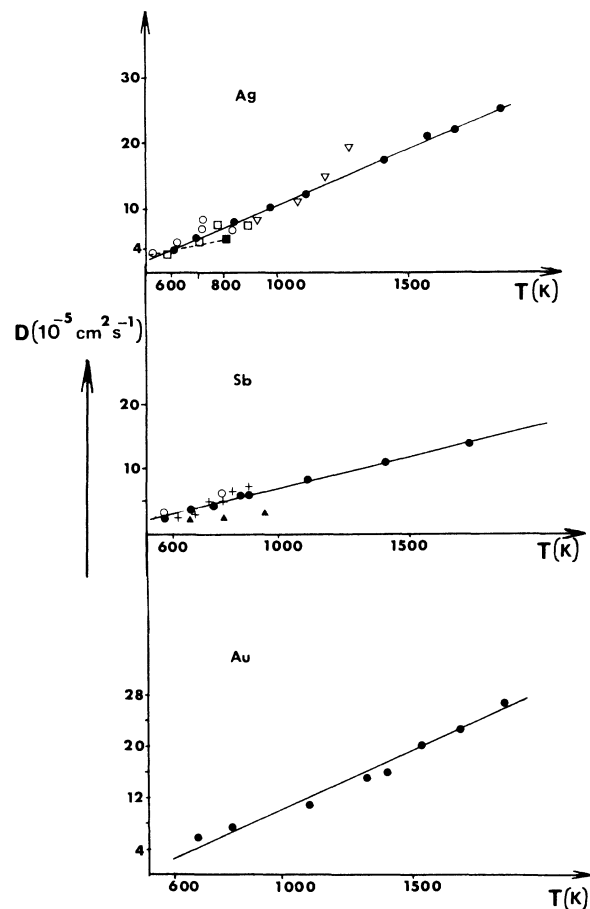


FIG. 1. Comparison of experimental diffusion coefficients of  $^{110m}\text{Ag}$ ,  $^{124}\text{Sb}$ , and  $^{195}\text{Au}$  in liquid Sn with those given by different authors: ---- Davis (Ref. 5),  $\nabla$  Tychina (Ref. 6),  $\blacksquare$  Golovchenko (Ref. 7),  $\square$  Kharkov (Ref. 8),  $\circ$  Teillier (Ref. 9),  $\blacktriangle$  Foster (Ref. 10),  $+$  Du Fou (Ref. 11),  $\bullet$  this work.

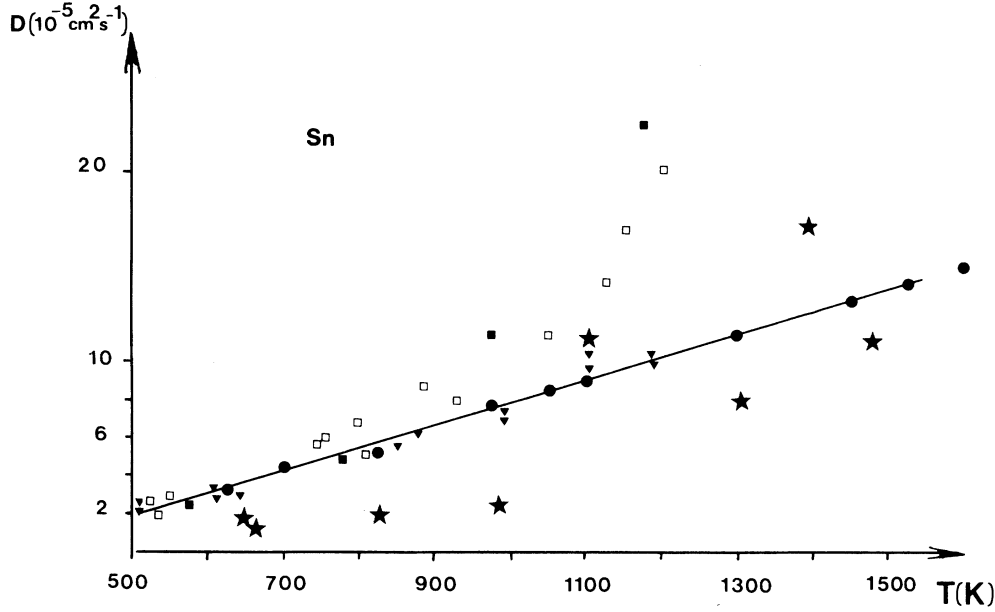


FIG. 2. Comparison of experimental self-diffusion coefficients in liquid Sn with the data of different authors: ■ Kharkov (Ref. 12), □ Ma and Swalin (Ref. 13), ★ Foster (Ref. 10), ▲ Davis and Fryzuck (Ref. 14), ● this work.

$T$ , and we assume that their values remain unaltered in a dilute alloy.

### B. Radial distribution function

From the work of Lebowitz<sup>18</sup> the radial distribution functions (RDF)  $g_{ii}$ ,  $g_{ss}$ , and  $g_{is}$  are obtained through an extension of the Percus-Yevick theory to multicomponent systems. The RDF are functions of the hard-sphere diameters and of the partial-packing fractions  $y_i$  and  $y_s$  of the solute and solvent, respectively,

$$g_{ii}(\sigma_i) = \frac{1}{(1-y)^2} \left[ \left(1 + \frac{1}{2}y\right) + \frac{1}{2}(y_s/\sigma_s)(\sigma_i - \sigma_s) \right],$$

$$g_{is}(\sigma_{is}) = \frac{1}{2\sigma_{is}} [\sigma_i g_{ss}(\sigma_s) + \sigma_s g_{ii}(\sigma_i)],$$
(5)

where  $y = y_i + y_s$  is the packing fraction of the binary mixture and  $g_{ss}(\sigma_s)$  is obtained from  $g_{ii}(\sigma_i)$  by interchanging  $g_{ss}$ ,  $\sigma_s$  with  $g_{ii}$ ,  $\sigma_i$ . As it stands the expression for  $g_{is}(\sigma_{is})$  can be introduced in Eq. (3) to obtain  $D_i^E$ . However, it is well known that the Carnahan-Starling equation of state for binary hard-sphere liquids is more accurate than the Percus-Yevick equation of state. Therefore we replace the factor  $(1-y)^{-2}$  involved in the expressions of  $g_{ii}$  and  $g_{is}$  by the factor  $(2-y)/[(2+y) \times (1-y)^3]$ , which makes sure that the resulting expressions for the radial distribution functions are compatible with the Carnahan-Starling equation of state. Using this procedure we obtain the following expression for  $g_{is}(\sigma_{is})$ :

$$g_{is}(\sigma_{is}) = \frac{(2-y)}{(2+y)(1-y)^3} \times \left( 1 + \frac{y}{2} - \frac{3}{4\sigma_{is}} (\sigma_i - \sigma_s)(y_i - y_s) \right),$$
(6)

which is introduced in Eq. (3) to give  $D_i^E$ .

This equation is obtained in the frame of the Enskog approximation, which neglects correlated collisions between diffusing species. Apart from the work of Résibois,<sup>19</sup> Mehaffey and Cukier,<sup>20</sup> and Hynes, Kapral, and Weinberg,<sup>21</sup> there is no analytic or semianalytic description of these correlations. We therefore prefer, as we did in Ref. 1, to rely on molecular dynamics calculations for estimating these correlation effects.

### C. Dynamic correlations

The difference between the diffusion coefficient  $D_i$  obtained experimentally and the binary collision diffusion coefficient  $D_i^E$  calculated using Enskog's theory can be attributed to dynamic correlations, which are completely ignored in the

TABLE II. Values of the parameters  $A$  and  $D_m$  [Eq. (2)] for the diffusion of  $^{110m}\text{Ag}$ ,  $^{113}\text{Sn}$ ,  $^{124}\text{Sb}$ , and  $^{195}\text{Au}$  in liquid Sn.

	$^{110m}\text{Ag}$	$^{113}\text{Sn}$	$^{124}\text{Sb}$	$^{195}\text{Au}$
$A$ ( $10^{-8} \text{ cm}^2 \text{ s}^{-1} \text{ K}^{-1}$ )	17.2	12	10.6	17.7
$D_m$ ( $10^{-5} \text{ cm}^2 \text{ s}^{-1}$ )	2.07	1.80	2.23	1.30

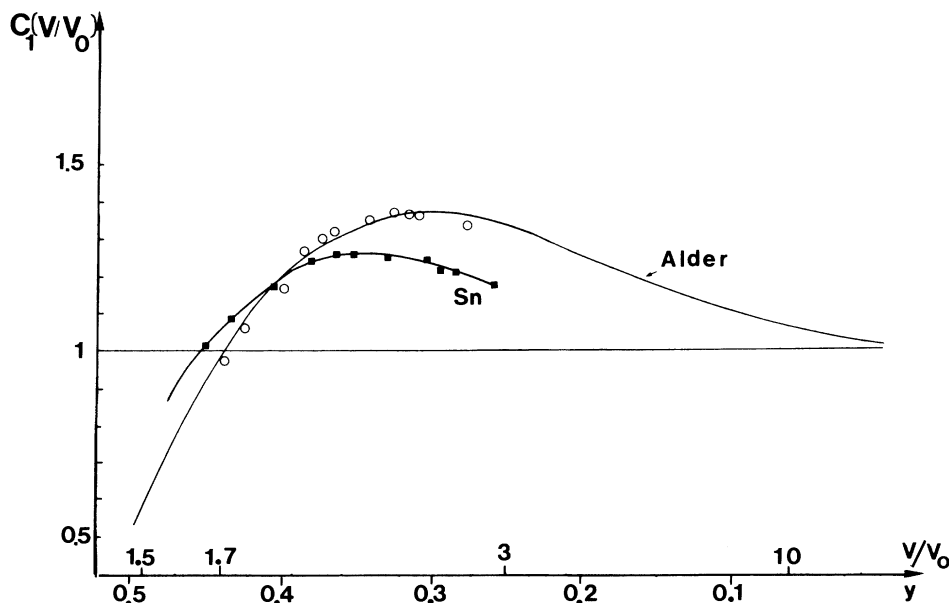


FIG. 3. Experimental ratio  $D_s/D_s^E = C_1(V/V_0)$  in Sn (squares) compared with Alder's data (Ref. 3).  $D_s/D_s^E$  calculated with the effective hard-sphere diameter given by Eq. (9) (points).

Enskog description. According to the computer simulations made by Alder *et al.*,<sup>3,4</sup> these correlations depend strongly on the solvent density, as well as on the relative size and mass of the solute with respect to the solvent. Using our experimental results and the binary collision diffusion coefficient calculated in a hard-sphere system, we can estimate a correction factor due to dynamic correlations and compare its value to that predicted by numerical simulation. In what follows we discuss separately density effects and the influence of the mass and of the size of the solute atoms.

### 1. Density effects

Density effects are most easily discussed when self-diffusion results are considered. The binary collision self-diffusion coefficient  $D_s^E$  can be written

$$D_s^E = \frac{3}{8n\sigma_s^2 g_s(\sigma_s)} \left( \frac{kT}{\pi m_s} \right)^{1/2},$$

where  $g_s(T)$  is given by Eq. (4) and

$$g_s(\sigma_s) = \frac{(2-y)}{2(1-y)^3},$$

$$y = \frac{1}{6} \pi \sqrt{2} \left( \frac{V}{V_0} \right)^{-1}.$$

In what follows we assume that the temperature dependence of the self-diffusion coefficient is contained in  $D_s^E$  and that the ratio

$$C_1 \left( \frac{V}{V_0} \right) = \frac{D_s}{D_s^E} \quad (7)$$

is a function of the density only and represents the departure of  $D_s$  from the binary collision diffusion coefficient  $D_s^E$ .

The values of  $C_1$  obtained using this procedure are represented in Fig. 3 and compared with theoretical values obtained by Alder<sup>3</sup> in hard-sphere systems. Qualitatively, the overall agreement is fairly good (i) at high densities ( $1.5 < V/V_0 < 1.7$ ), the backscattering regime is predominant and leads to a value of  $C_1$  which is smaller than unity and (ii) in the intermediate density range ( $V/V_0 \sim 3$ ),  $C_1$  is larger than unity, which can be traced to persistence effects induced by the initial motion of a given atom. As shown by Alder<sup>22</sup> it is likely that the test particle initiates long-wavelength hydrodynamic motions which decay slowly, which explains the long-time tail in the velocity autocorrelation function and the increase of the diffusion coefficient with respect to its value in the Enskog approximation.

In a second step in our interpretation, we assume that the values  $C_1'$  of  $C_1$  calculated by Alder are exact and we determine the value of the effective hard-sphere diameter  $\sigma_s'(T)$  which would give the Enskog coefficient

$$D_s'^E = \frac{D_s}{C_1'}.$$

We find that, instead of the value of  $\sigma_s(T)$  given by

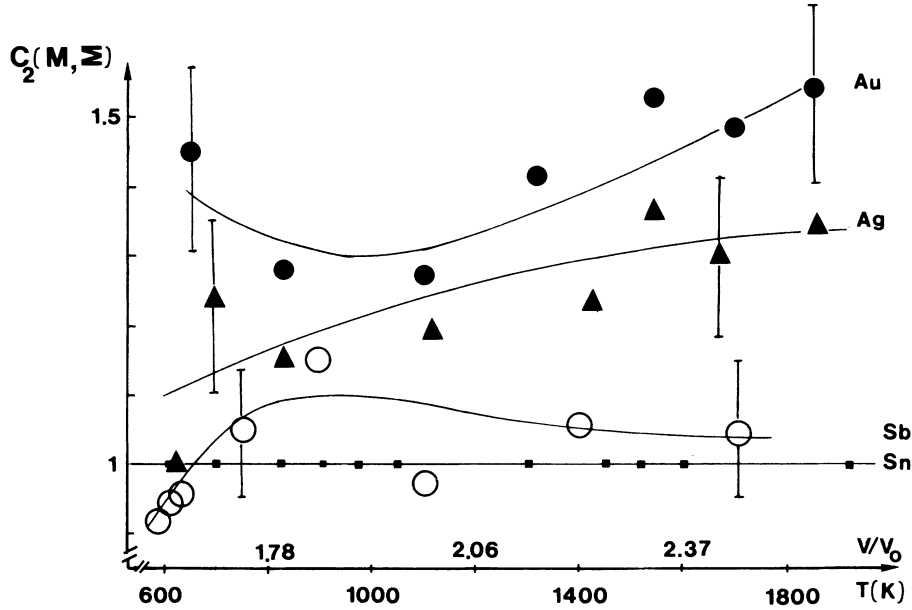


FIG. 4. Experimental values of  $C_2(M, \Sigma)$  for  $^{110m}\text{Ag}$ ,  $^{195}\text{Au}$ ,  $^{124}\text{Sb}$ , and  $^{113}\text{Sn}$  according to Eq. (12).

Protopapas,

$$\sigma_s(T) = 3.30[1 - 0.112(T/T_m)^{1/2}] \quad (8)$$

and corresponding to the packing fraction  $y_m = 0.472$  at the melting point, we must use

$$\sigma'_s(T) = 3.17[1 - 0.082(T/T_m)^{1/2}], \quad (9)$$

in order to recover the results predicted by molecular dynamics calculations. The values of  $\sigma'_s(T)$  differ by at most 3% from that of  $\sigma_s(T)$  in the temperature range investigated in the present work, and correspond to a packing fraction  $y'_m = 0.455$  at the melting point. The values of  $\sigma'_s(T)$  must not be taken too seriously, however, because the dynamical properties of liquid tin are not necessarily accurately represented using an equivalent hard-sphere system.

## 2. Impurity diffusion—mass and size effects

Once the binary collision diffusion coefficient  $D_i^E$  for impurity diffusion has been calculated using Eq. (3), we assume that the ratio

$$C_i = \frac{D_i}{D_i^E} \quad (10)$$

is a function of the density of the fluid and of the ratios  $M = m_i/m_s$  and  $\Sigma = \sigma_i/\sigma_s$  of the solute- and solvent-mass and size, respectively. As our experiments have been made in very dilute alloys, we can assume that the dependence of  $C_i$  on density is the same as that found in self-diffusion.

Therefore we can write

$$C_i((V/V_0), M, \Sigma) = C_1(V/V_0)C_2(M, \Sigma) \quad (11)$$

where  $C_1(V/V_0)$  is given by the Eq. (7). Using this procedure, we can calculate at each temperature the correction factor

$$C_2(M, \Sigma) = \frac{D_i}{D_i^E} \frac{D_s^E}{D_s}, \quad (12)$$

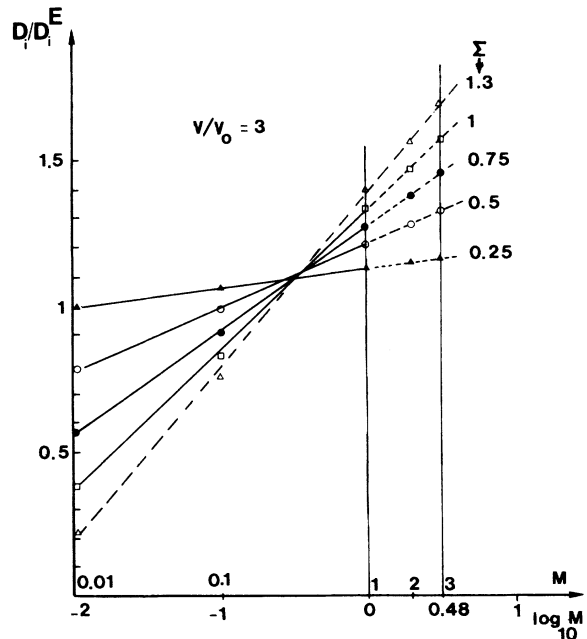


FIG. 5. Variation of  $D_i/D_i^E$  as a function of  $\log_{10} M$ , for various size ratios  $\Sigma$ . —: interpolation of Alder's results; - - - -: extrapolation of Alder's data to  $(M, \Sigma) > (1, 1)$ .

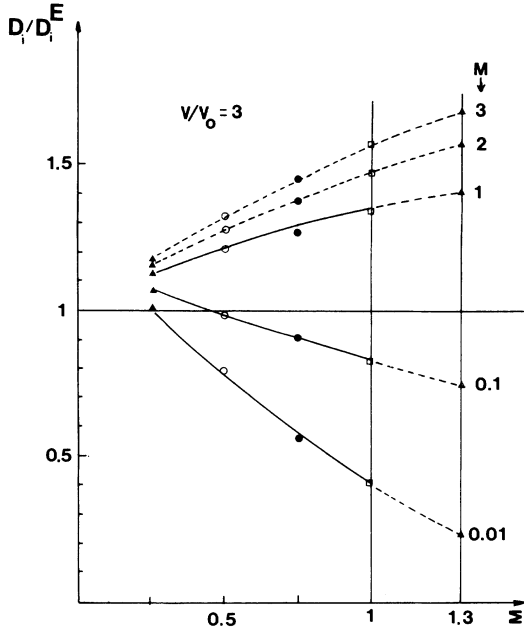


FIG. 6. Variation of  $D_i/D_i^E$  as a function of  $\Sigma$  at constant  $M$ . —: Alder's data; ----: extrapolation of Alder's data to  $(M, \Sigma) > (1, 1)$ .

which is represented in Fig. 4 for  $^{110m}\text{Ag}$ ,  $^{195}\text{Au}$ ,  $^{124}\text{Sb}$ , and  $^{113}\text{Sn}$  in Sn.

Molecular dynamics calculations have been made by Alder *et al.*<sup>4</sup> on hard-sphere systems with  $(M, \Sigma) \leq (1, 1)$ . It is therefore necessary to extrapolate these results to the range  $(M, \Sigma) \geq (1, 1)$  in order to make a comparison with our experimental results. This extrapolation is made using the same method as that used by Protopapas.<sup>23</sup> For instance, at the density corresponding to  $V/V_0 = 3$ , we mention these points: (i) We note (Fig. 5) that in the range  $M \leq 1$ , the values of  $D_i/D_i^E$  calculated by Alder vary linearly as a function of  $\log_{10} M$  whatever the size ratio  $\Sigma$ . It is therefore possible to extrapolate these results up to  $M = 3$ , and we think that the values of  $C_i = D_i/D_i^E$  obtained in this way do not depart drastically from what would be obtained in a detailed computer calculation. (ii) We use the same procedure to obtain  $C_i$  for values of  $\Sigma$  up to 1.3 (Fig. 6). Using the value of  $C_1(V/V_0)$  given by  $C_i(V/V_0, 1, 1)$  we obtain "theoretical values" of  $C_2(M, \Sigma)$  which are reported in Table III for  $V/V_0 = 3$  and 1.6.

It is now possible to compare the experimental value  $C_2^{\text{expt}}$  of  $C_2$  given by the Eq. (12) to the theo-

TABLE III. Values of  $C_i = D_i/D_i^E$  interpolated and extrapolated from Alder's data (Ref. 4) and values of  $C_2^{\text{theor}} = C_i/C_i(V/V_0, 1, 1)$  calculated for  $V/V_0 = 3$  and 1.6.  $C_2^{\text{expt}}$  denotes the experimental values obtained by Eq. (12) for Ag, Au, Sn, and Sb in liquid tin.

Solute	$\Sigma$	$M$	$V/V_0 = 3$			$V/V_0 = 1.6$		
			$C_i = D_i/D_i^E$	$C_2^{\text{theor}} = \frac{C_i}{C_i(V/V_0, 1, 1)}$	$C_2^{\text{expt}} (V/V_0 = 2.6)$	$C_i = D_i/D_i^E$	$C_2^{\text{theor}} = \frac{C_i}{C_i(V/V_0, 1, 1)}$	$C_2^{\text{expt}}$
Ag	0.75	0.1	0.91	0.68		0.47	0.6	
		0.9	1.25	0.94		0.81	1.04	
		1	1.27	0.95		0.83	1.06	
		2	1.37	1.03		0.91	1.17	
		3	1.46	1.10		0.97	1.24	
Ag	0.9	0.1	0.86	0.65		0.43	0.55	
		0.9	1.29	0.97	1.30	0.78	1.00	1.10
		1	1.31	0.98		0.80	1.03	
Au	1.7	1.40	1.05	1.49	0.86	1.10	1.38	
		2	1.43	1.08		0.87	1.12	
		3	1.52	1.14		0.93	1.19	
Sn	1	0.1	0.82	0.62		0.40	0.51	
		0.9	1.31	0.98		0.76	0.97	
		1	1.33	1.00	1.00	0.78	1.00	1.00
Sn	2	1.43	1.09		0.86	1.10		
		3	1.55	1.17		0.92	1.18	
		1.03	1.05	1.36	1.02	1.04	0.80	1.03
Sb	1.3	0.1	0.75	0.56		0.37	0.47	
		0.9	1.38	1.04		0.71	0.91	
		1	1.40	1.05		0.73	0.94	
		2	1.57	1.18		0.83	1.06	
		3	1.68	1.26		0.89	1.14	

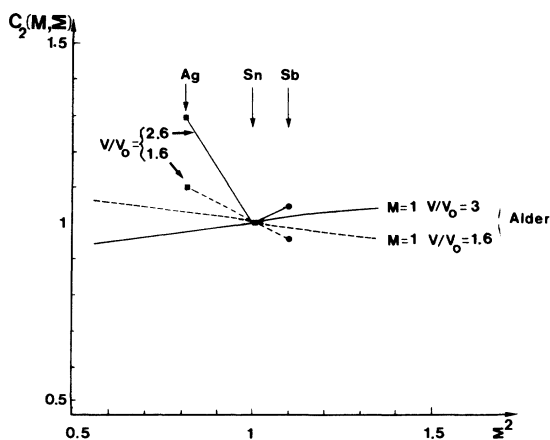


FIG. 7. Variation of  $C_2^{\text{expt}}$  and  $C_2^{\text{theor}}$  with  $\Sigma^2$  at two different densities  $V/V_0=3$  (—),  $V/V_0=1.6$  (----).

retical value  $C_2^{\text{theor}}$ . This comparison is made in Table III as a function of  $M$  and  $\Sigma$ . It can be noted that both experiment and calculations exhibit the same  $M$  dependence of  $C_2$ ;  $C_2$  increases as the mass of the solute atom increases from Ag to Au, whatever the density. This behavior is easy to understand for the following reasons: (i) at high density the backscattering effect decreases when the mass of the solute increases and (ii) at intermediate density, a heavy test particle is more efficient for inducing hydrodynamic modes than a light particle. Let us also note that the agreement between  $C_2^{\text{expt}}$  and  $C_2^{\text{theor}}$  would be quantitatively very much better if, instead of approximating  $C_i(V/V_0)$  by  $D_s/D_s^E$ , we had used the value  $C_i(V/V_0, 1, 1)$  obtained by Alder.

In Fig. 7 we have reported the values of  $C_2^{\text{expt}}$  and  $C_2^{\text{theor}}$  as a function of  $\Sigma^2$  at two different densities ( $V/V_0=1.6, 3$ ). At the density corresponding to  $V/V_0=1.6$ , both  $C_2^{\text{expt}}$  and  $C_2^{\text{theor}}$  decrease when  $\Sigma$  increases from Ag to Sb. At smaller densities

( $V/V_0 \approx 3$ ), however, it can be seen in Fig. 7 that  $C_2^{\text{expt}}$  is larger than  $C_2^{\text{theor}}$  for impurities smaller (Ag) or larger (Sb) than Sn. For the Sb solute,  $C_2^{\text{expt}}$  is larger than unity, as can be predicted using Alder's results. A more challenging result is that  $C_2^{\text{expt}}(\text{Ag})$  is much larger than unity, whereas  $C_2^{\text{theor}}(\text{Ag})$  is smaller than unity for the density  $V/V_0=3$ . This can be due to valence effects: For an impurity whose valence is different from that of the solvent, the RDF at contact may be very different from the values calculated using hard spheres. Moreover, the local density of the fluid around the impurity can be changed from its mean value and, as  $C_i$  depends strongly on  $V/V_0$ , this may affect considerably the velocity autocorrelation function of the impurity. Some calculations are now in progress to settle this point.

#### IV. CONCLUSION

We have measured the diffusion coefficients of  $^{110m}\text{Ag}$ ,  $^{113}\text{Sn}$ ,  $^{124}\text{Sb}$ , and  $^{195}\text{Au}$  in liquid tin using a shear cell assembly which provides data with a precision of about 5%. From the density effect on the self-diffusion coefficient of Sn, we have been able to determine an effective hard-sphere diameter of Sn in a large temperature range. At large densities, the correction factor to Enskog's theory decreases as the mass of the solute decreases, as predicted by molecular dynamics calculations. Size effects on the correlation factor do not exhibit the same trend as in calculations, especially for smaller impurities. As our interpretations are essentially based on calculations made on hard-sphere systems, it would be very interesting (i) to calculate the binary collision diffusion coefficient of Sn using realistic potentials and (ii) to calculate the diffusion coefficient of impurities in Sn using interatomic potentials deduced from liquid-alloy theory.

\*Laboratoire associé au C.N.R.S. No. 155.

<sup>1</sup>A. Bruson and M. Gerl, Phys. Rev. B **19**, 6123 (1979).

<sup>2</sup>S. Chapman and T. G. Cowling, *The Mathematical Theory of Nonuniform Gases* (Cambridge University, New York, 1970).

<sup>3</sup>B. J. Alder, D. M. Gass, and T. E. Wainwright, J. Chem. Phys. **53**, 3813 (1970).

<sup>4</sup>B. J. Alder, W. E. Alley, and J. M. Dymond, J. Chem. Phys. **61**, 1415 (1974).

<sup>5</sup>K. G. Davis and P. Fryzuck, Trans. A.I.M.E. **233**, 1662 (1965).

<sup>6</sup>J. I. Tychina and T. V. Vasilenko, Izv. Akad. Nauk. S.S.R. Metall. **4**, 101 (1972).

<sup>7</sup>V. G. Golovchenko, T. V. Vasilenko, and F. P. Golotyuk, Vis. Kiev. Univ. Ser. Fiz. **9**, 27 (1968).

<sup>8</sup>E. I. Kharkov, A. P. Zvyagintsev, and G. I. Onoprienko,

Ukrainsk. Fiz. Zh. **15**, 1733 (1970).

<sup>9</sup>A. Teillier, thesis, Grenoble, France, 1971 (unpublished).

<sup>10</sup>J. P. Foster and A. J. Reynick, Met. Trans. **4**, 207 (1973).

<sup>11</sup>M. O. du Fou, thesis, Nancy, France, 1975 (unpublished).

<sup>12</sup>E. I. Kharkov, A. P. Zvyagintsev, and G. I. Onoprienko, Fiz. Metal. Metalloved. **31**, 220 (1971).

<sup>13</sup>C. H. Ma and R. A. Swalin, Acta Metallogr. **8**, 388 (1960).

<sup>14</sup>K. G. Davis and P. Fryzuck, J. Appl. Phys. **39**, 4848 (1968).

<sup>15</sup>G. Jacucci and I. R. McDonald, Physica A **80**, 607 (1975).

<sup>16</sup>P. Protopapas, H. C. Andersen, and N. A. D. Parlee,

- J. Chem. Phys. 59, 15 (1973).
- <sup>17</sup>P. Protopapas and N. A. D. Parlee, Chem. Phys. 11, 201 (1975).
- <sup>18</sup>J. L. Lebowitz, Phys. Rev. A 133, 895 (1975).
- <sup>19</sup>P. Resibois, J. Stat. Phys. 13, 393 (1975).
- <sup>20</sup>J. R. Mehafeff and R. I. Cukier, Phys. Rev. A 17, 1181 (1978); R. I. Cukier and J. R. Mehafeff, Phys. Rev. A 18, 1202 (1979).
- <sup>21</sup>J. T. Hynes, R. Kapral, and M. Weinberg, J. Chem. Phys. 70, 1456 (1979).
- <sup>22</sup>B. J. Alder and T. E. Wainwright, Phys. Rev. A 1, 18 (1970).
- <sup>23</sup>P. Protopapas and N. A. D. Parlee, High Temp. Sc. 8, 141 (1976).